Bulletin of Engineering Geology and the Environment (2019) 78:1697–1708
https://doi.org/10.1007/s10064-017-1201-6

ORIGINAL PAPER

Evaluation of soil liquefaction potential using energy approach: experimental and statistical investigation

Hamed Javdanian [1]

Received: 27 June 2017 / Accepted: 6 November 2017 / Published online: 22 November 2017

Abstract
Liquefaction has caused many catastrophes during earthquakes in the past . The strain energy-based method is one of the modern methods used to estimate liquefaction potential. In this study, wide-ranging experimental data were gathered from cyclic tests and centrifuge modeling of liquefaction. A model was then developed based on the strain energy needed for liquefaction to occur using the group method of data handling and the gravitational search algorithm. Contributions of the effective variables were evaluated through a sensitivity analysis. To check the accuracy of the developed strain energy model, cyclic triaxial tests were conducted on sandy soil and silty sand specimens. Comparison of the energy required to initiate liquefaction in the tested soil specimens with values predicted by the developed model indicated high accuracy of the energy-based model. Subsequently, the accuracy of the energy model was assessed in field conditions using the amount of strain energy released by real earthquakes in various sites. The ability of the model to distinguish liquefied areas from non-liquefied ones confirms its accuracy in field conditions. Finally, the developed model was compared with some available relationships to estimate the strain energy required for liquefaction to occur.

Keywords Liquefaction · Earthquake · Strain energy · Cyclic triaxial test · GMDH

Introduction

Earthquakes can cause a lot of geotechnical damage, including the phenomenon of liquefaction (Ishihara 1996; Sonmez and Ulusay 2008; Zhuang et al. 2016). Liquefaction occurs when saturated soil loses strength due to the earthquake loading and increased pore water pressure (Papathanassiou et al. 2011; Javdanian and Hoseini 2016; Mehrzad et al. 2016; Javdanian and Seidali 2016). Traumatic experiences from this phenomenon has stimulated researchers to use various methods to estimate the potential for liquefaction (e.g., Kaveh et al. 2016; Rahman and Siddiqua 2017). Models based on strain energy (W) absorption in soils are amongst the newest methods for estimation of liquefaction potential (Baziar et al. 2011; Jafarian et al. 2012). In the strain energy method, liquefaction within the critical state framework occurs with the arrival of a seismic wave of energy exceeding a certain threshold that represents the liquefaction potential of the soil deposit in terms of energy.

The stress-based method (Youd et al. 2001; Seed and Idriss 1971; Whitman 1971) and strain-based method (Dobry et al. 1982) are common techniques for the estimation of liquefaction potential (Baziar and Jafarian 2007). In these methods, the generation of pore water pressure and subsequently liquefaction incidence is correlated with the amount of seismic shear stresses and shear strains in the soil, respectively. In fact, the energy-based method relates the incidence of liquefaction to the levels of stress and strain induced by cyclic loading. Therefore, the strain energy method is physically more realistic than these other two techniques (Kokusho and Mimori 2015). The quantity of energy needed for the initiation of liquefaction is obtained from experimental results or field data. The area inside the hysteresis loop (the shear stress-shear strain curve) indicates the amount of dissipated strain energy at the unit volume of the soil mass (Figueroa et al. 1994; Jafarian et al. 2011). The total amount of this strain energy needed for the occurrence of liquefaction is equal to the amount of strain energy needed for initiation of this phenomenon. The existence of more accurate models for estimation of this amount of strain energy reduces uncertainty in the estimation of liquefaction potential.

✉ Hamed Javdanian
javdanian@eng.sku.ac.ir

[1] Department of Civil Engineering, Shahrekord University, Shahrekord, Iran

In recent years, novel appearance of optimization, modeling, and problem solving have evolved regarding the pervasive progress in computational approaches. These aspects are referred as soft computing-based methods and are very powerful methods for multivariate and non-linear modeling (Javdanian 2017). Soft computing-based techniques such as artificial neural networks (Baziar and Jafarian 2007; Caglar and Arman 2007; Javdanian et al. 2012; Jafarian et al. 2014; Mohammadi et al. 2015), genetic programming (Baziar et al. 2011), linear genetic programming (Alavi and Gandomi 2012), multi-expression programming (Alavi and Gandomi 2012), adaptive neuro-fuzzy inference systems (Javdanian et al. 2015b; Li et al. 2017; Javdanian 2017), multivariate adaptive regression splines (Zhang and Goh 2013, 2016; Goh and Zhang 2014), and support vector machines (Xue and Yang 2016) have contributed widely to the various topics of geotechnical engineering. In recent years, the group method of data handling (GMDH)-based networks have provided successful evaluations in problems associated with soils (e.g., Kalantary et al. 2009; Najafzadeh et al. 2013; Javdanian et al. 2015a; Najafzadeh and Tafarojnoruz 2016; Javdanian et al. 2017).

In the present research, a neuro-fuzzy GMDH (NF-GMDH) model was developed for evaluation of the soil liquefaction potential. For this purpose, a comprehensive database of cyclic laboratory tests was applied to develop a strain energy-based model. Also, the gravitational search algorithm (GSA) was used in a topology plan of the NF-GMDH-based model for evaluation of the triggering of liquefaction. In addition, the applicability of the proposed model was assessed using centrifuge data. A sensitivity analysis was carried out to evaluate the behavior of the developed model in relation to the variation of influential parameters. To evaluate the performance of the NF-GMDH-GSA-based model, cyclic triaxial tests were conducted on sandy soil and silty sand specimens and the test results were compared with the values obtained from the proposed energy model. Performance of the developed model was appraised in field conditions using the real strain energy released by earthquakes in different regions. Finally, a comparison was carried out between the performance of the developed model and some available recommendations.

Database of cyclic tests and centrifuge modeling

With the progression of cyclic laboratory tests on soil specimens and assessment of dynamic soil behavior, considerable data have now been gathered and there is now a wide-ranging database for sands and silty sands. In our research, available laboratory data were re-analyzed and an effort was made to suggest a statistical model for predicting the strain energy required for triggering of soil liquefaction. A relatively large database (consisting of 424 datasets) was gathered from the available experimental tests performed by Towhata and Ishihara (1985), Arulmoli et al. (1992), Liang (1995), Rokoff (1999), Green (2001), Tao (2003), Kanagalingam (2006), and Jafarian et al. (2012). Table 1 summarizes the main features of these experimental programs. These tests were conducted on sands and silty sands by cyclic torsional shear, cyclic triaxial, and cyclic simple shear apparatuses. For validation of the performance of developed model, the centrifuge tests results (Dief 2000) (Table 1) were also used as validation dataset.

Influential parameters

A thorough understanding of the factors affecting the cyclic behavior of soils is required to obtain the precise strain energy needed for liquefaction occurrence. The experimental findings of Towhata (1986) and Figueroa et al. (1994) showed that the effective confining pressure (σ'_0) and relative density (D_r) have significant effect on the strain energy needed for soil liquefaction. The influence of these parameters on the liquefaction potential of soils has been confirmed by other researchers (e.g., Seed and Lee 1966; Jafarian et al. 2010). The experimental and field studies indicate the significant effect of fines content (FC) on the behavior of cyclic soils (Naeini and Baziar 2004; Chien et al. 2002; Thevanayagam 1998; Baziar and Dobry 1995). Moreover, extensive studies were conducted on the effect of particle size on the cyclic resistance of soils (e.g., Liang 1995; Lee and Fitton 1968). Results showed that the cyclic resistance of sandy soils is affected by characteristics of particle size distribution such as coefficient of uniformity (C_u) and mean particle size (D_{50}) (Rokoff 1999; Lee and Fitton 1968). Baziar and Jafarian (2007) showed that the use of coefficient of curvature (C_c) does not improve the accuracy of liquefaction potential estimation. Therefore, this study used five parameters including D_r, mean initial effective confining stress (σ'_0), FC, mean grain size (D_{50}), and C_u to estimate the strain energy required for soil liquefaction triggering. The characteristics of the influential parameters on the collected experimental results are presented in Table 1.

Model descriptions

Neuro-fuzzy group method of data handling (NF-GMDH)

The GMDH-based network is machine learning tool for decision making and classification; it is a kind of artificial neural network with polynomial activation function. The model converges to a termination criterion after a sufficient number of epochs using series of embedded operations (Madala and Ivakhnenko 1994). Various extensions of this network have been addressed in the literature (e.g., Hwang 2006). One of the well-known extensions is called NF-GMDH, which is constructed automatically by a self-organized algorithm (Hwang

Table 1 Summary of soil characteristics compiled in the database

Study	Testing apparatus	Soil type	σ'_0 (kPa)	D_r (%)	FC (%)	C_u	D_{50} (mm)	W (J/m^3)
Towhata and Ishihara (1985)	Cyclic torsional	Toyoura sand	294	43.1–50.7	0	1.57	0.19	5000–6300
Arulmoli et al. (1992)	Cyclic simple shear, cyclic triaxial	Nevada sand	40–160	41.6–62.7	0	2.27	0.15	398.2–10,868
Liang (1995)	Cyclic torsional	Reid Bedford sand	41.1–124.1	48.6–75.5	0	1.67	0.26	593–2737
	Cyclic torsional	LSFD sand	41.1–124.1	57.2–91.7	28	5.88	0.13	517–1379
	Cyclic torsional	LSI-30 sand	41.1–124.1	49.1–71.9	0	2.39	0.39	839–4098
Rokoff (1999)	Cyclic torsional	Nevada sand	46.2–141.3	42.6–71.1	0	2.27	0.15	466–6238
Green (2001)	Cyclic triaxial	Monterey sand and silty sand	93.74–101.4	−4.7 – 98.3	0–75	1.63–1.87	0.14–0.46	480–34,970
	Cyclic triaxial	Yatesville sand and silty sand	95.32–103.1	−44.5 – 105.1	0–100	2.44–4.44	0.03–0.17	300–8320
Tao (2003)	Cyclic torsional	LSFD sand–silt mixtures	41.1–124.1	44–78	0–45	1.88–9.19	0.09–0.15	789–7130
Kanagalingam (2006)	Cyclic triaxial	Ottawa sand–silt mixtures	100–400	9.38–91.78	0–60	1.52–28.12	0.03–0.23	590–15,000
Jafarian et al. (2012)	Cyclic hollow cylinder torsional	Toyoura sand	55–166	29.26–76.93	0	1.5	0.2	415–6032
Dief (2000)	Centrifuge tests	Nevada sand	28.4–34.7	58.5–76.3	0	2.27	0.15	590–1405
		Reid Bedford sand	28.8–34.6	51–80.4	0	1.67	0.26	550–1680
		LSFD sand	14.1–32.3	55–93	28	5.88	0.13	385–508

C_u coefficient of uniformity, *D_{50}* mean particle size, *D_r* relative density after consolidation, *FC* fines content, *W* strain energy, *σ'_0* confining pressure, *LSFD* Lower San Fernando Dam

2006; Najafzadeh and Azamathulla 2013). Evolutionary algorithms adapt easily with the NF-GMDH algorithm due to its high flexibility. In addition, a simplified fuzzy reasoning rule such as "If x_1 is equal to F_{k1} and x_2 is equal to F_{k2}, output y is equal to w_k" is used to improve the GMDH network (Takashi et al. 1998). The function of Gaussian membership is employed in terms of F_{kj} which is associated with the kth fuzzy rules in the extent of the jth input values x_j (Eq. 1):

$$F_{kj}(x_j) = exp\left(-\frac{(x_j - a_{kj})^2}{b_{kj}}\right) \tag{1}$$

where a_{kj} and b_{kj} are the constant amounts for each fuzzy rule. Also, the y parameter is specified as an output, which has been represented as Eqs. 2 and 3:

$$y = \sum_{k=1}^{K} u_k w_k \tag{2}$$

$$u_k = \prod_j F_{kj}(x_j) \tag{3}$$

where w_k is the real value for kth rules (Najafzadeh and Lim 2014; Hwang 2006; Takashi et al. 1998).

In the NF-GMDH model, each neuron has two input variables and one output variable. The output of each neuron in a layer is directly connected to the input entry of the next layer. Calculating the average of the outputs from the last layer, the final output is obtained. The inputs variables from the mth model and pth layer are the output variables of the $(m-1)$-th and m-th model in the $(p-1)$-th layer. The mathematical functions to compute y^{pm} are as follows (Eqs. 4 and 5):

$$y^{pm} = f\left(y^{p-1,m-1}, y^{p-1,m}\right) = \sum_{k=1}^{K} \mu_k^{pm}.w_k^{pm} \tag{4}$$

$$\mu_k^{pm} = exp\left\{-\frac{\left(y^{p-1,m-1} - a_{k,1}^{pm}\right)^2}{b_{k,1}^{pm}} - \frac{\left(y^{p-1,m} - a_{k,2}^{pm}\right)^2}{b_{k,2}^{pm}}\right\} \tag{5}$$

where μ_k^{pm} is the kth Gaussian function and w_k^{pm} is its corresponding weight param,eter, which are related to the mth model at the pth layer. Furthermore, a_k^{pm} and b_k^{pm} are the Gaussian parameters which are used for the ith input variable from the mth model and pth layer. Also, the final output variable is represented by Eq. 6:

$$y = \frac{1}{M}\sum_{m=1}^{M} y^{pm} \tag{6}$$

The process of learning of feedforward NF-GMDH is an iterative procedure for solving complicated systems. The error parameter, in each iteration, can be determined as Eq. 7:

$$E = \frac{1}{2}\left(y^* - y\right)^2 \tag{7}$$

where y^* is the predicted value.

NF-GMDH development using a gravitational search algorithm

One of the useful swarm intelligence algorithms is GSA, which explores in a multidimensional search space for extremum values of target function. In this algorithm, optimization is performed on the basis of the gravity rule and movement in an artificial system with discrete time coordinates (Rashedi et al. 2009). According to GSA, a collection of masses turns into search agents, in a way in which every mass can percept the location and position of other masses. Therefore, the information is transferred between different masses using the gravitational force.

In GSA, for a minimization problem, the mass of each agent is computed after calculating the current population fitness (Najafzadeh and Lim 2014; Rashedi et al. 2009) (Eqs. 8 and 9):

$$q_i(t) = \frac{fit_i(t) - worst(t)}{best(t) - worst(t)} \tag{8}$$

$$M_i(t) = \frac{q_i(t)}{\sum_{j=1}^{N} q_j(t)} \tag{9}$$

where $M_i(t)$ and $fit_i(t)$ stand for the mass and the fitness amount of agent i at time t; and N represents the population size. Also, for a minimization problem, $worst(t)$ and $best(t)$ are defined as follows (Eqs. 10 and 11:

$$best(t) = \min_{j \in \{1,\dots,N\}} fit_j(t) \tag{10}$$

$$worst(t) = \max_{j \in \{1,\dots,N\}} fit_j(t) \tag{11}$$

For calculating the acceleration of an agent, all forces from heavier masses applied to it should be computed by simultaneously considering the law of gravity and the second law of Newton on motion (Eq. 12) (Rashedi et al. 2009). After this, the updated velocity of an agent is obtained as a fraction of its current velocity added to its acceleration (Eq. 13). Then, its situation could be determined using Eq. 14.

$$a_i^d(t) = \sum_{j \in kbest, j \neq i} rand_j G(t) \frac{M_j(t)}{R_{i,j}(t) + \varepsilon} \left(x_j^d(t) - x_i^d(t) \right), \quad d = 1, 2, \dots, n \; ; \; i = 1, 2, \dots, N \tag{12}$$

$$v_i^d(t+1) = rand_i \times v_i^d(t) + a_i^d(t) \tag{13}$$

$$x_i^d(t+1) = x_i^d(t) + v_i^d(t+1) \tag{14}$$

where x_i^d, v_i^d and a_i^d stand for the position, velocity, and acceleration of agent i in dimension d, respectively. $rand_i$ and $rand_j$ are two uniform randoms at the range of [0, 1], ε is a small amount, n is the dimension of the search space, and $R_{i,j}(t)$ is the Euclidean distance between two agents i and j that were defined as $R_{i,j}(t) = \|X_i(t), X_j(t)\|_2$. It is noteworthy that $X_i = \left(x_i^1, x_i^2, \dots, x_i^n\right)$ expresses the position of ith agent in the search space. $kbest$ is the set of first K agents with the best fitness value and biggest mass, which is in terms of time, initialized to K_0 at the start and decreased by time. Here, K_0 is set to the total number of agents (N) and is decreased linearly to 1. G is a descending function of time, which is set to G_0 at the beginning and decreases exponentially with time as in Eq. 15:

$$G(t) = G_0 e^{-\alpha \frac{t}{T}} \tag{15}$$

In the optimization process, the values of G_0 and α are adjusted to 100 and 20, respectively. Also, the number of agents is 50 and the maximum number of iterations is 100. The GSA optimized coefficients of weighting in each neuron of the developed NF-GMDH network.

Data division

In machine learning procedures, as a usual method, the database is divided into two subsets: training and testing. The learning procedure is carried out using the training subset while the testing subset validates the trained predictive model. The data division method can impress the model efficiency (Shahin et al. 2004). In the present study, the dataset was distributed between training and testing subsets (Table 2) in a trial selection procedure, in which the main statistical parameters of two subsets (i.e., mean, maximum, minimum, and standard deviation) became close to each other. Eighty percent of the data (339 cyclic tests) were considered for the training and the rest of the data (85 cyclic tests) for the testing subset. Table 2 shows the statistical specifications of these subsets.

Performance measures

In order to assess the efficiency of developed models, mean absolute error (MAE), root mean squared error (RMSE), and the coefficient of determination (R^2) were calculated for the measured and predicted strain energy needed for liquefaction occurrence (Javdanian et al. 2015b). These are widely used statistical parameters for performance measurement (e.g., Jafarian et al. 2014). Theoretically, a predictive model with R^2 of unity and MAE and RMSE of zero is considered to be excellent. Also, the objective function (OBJ) (Eq. 16) (Gandomi et al. 2012; Najafzadeh and Azamathulla 2013) was used as a criterion of how well the predicted values agree

Table 2 Statistical analysis of inputs and output parameters of database

Variable	Dataset	Statistical parameters			
		Maximum	Minimum	Mean	Standard deviation
σ'_0 (kPa)	All data	400	40	102.92	49.99
	Training	400	40	101.79	43.77
	Testing	400	41.1	107.43	69.64
D_r (%)	All data	105.1	−44.5	51.7	29.28
	Training	105.1	−44.5	51.8	29.62
	Testing	96.8	−32.3	51.27	28.01
FC (%)	All data	100	0	17.95	23.99
	Training	100	0	18.01	24.38
	Testing	100	0	17.69	22.56
C_u	All data	28.12	1.5	4.02	5.97
	Training	28.12	1.5	4.09	6.08
	Testing	28.12	1.5	3.75	5.55
D_{50} (mm)	All data	0.46	0.029	0.211	0.11
	Training	0.46	0.029	0.212	0.11
	Testing	0.46	0.029	0.206	0.11
Log W (J/m^3)	All data	4.544	2.477	3.26	0.41
	Training	4.544	2.477	3.26	0.42
	Testing	4.44	2.69	3.25	0.38

C_u coefficient of uniformity, D_{50} mean particle size, D_r relative density after consolidation, FC fines content, W strain energy, σ'_0 confining pressure

with the measured experimental data. The best GMDH-based model was inferred by minimizing Eq. 16:

$$OBJ = \left(\frac{No._{tr} - No._{te}}{No._{all}}\right) \times \frac{RMSE_{tr} + MAE_{tr}}{R^2_{tr}} + \left(\frac{2 \times No._{te}}{No._{all}}\right) \times \frac{RMSE_{te} + MAE_{te}}{R^2_{te}} \quad (16)$$

where $No._{tr}$, $No._{te}$, and $No._{all}$ are the number of training, testing, and all datasets, respectively.

The OBJ captures the changes of MAE, RMSE, and R^2 together. Lower RMSE and MAE values and higher R^2 values result in lower OBJ and, consequently, indicate a more accurate model.

Results and discussion

In this study, several networks with different initial parameters were investigated, and the most accurate model was finally selected based on the calculated error parameters. The accuracy of the proposed model as determined by comparing the measured strain energy values (*Log W*) and those predicted by an NF-GMDH-GSA-based network is presented in Fig. 1a. The R^2, MAE, and RMSE values of the developed model for estimation of the strain energy required for liquefaction onset are 0.937, 0.024, and 0.036 in the training stage and 0.883, 0.040, and 0.051 in the testing stage, respectively. Moreover, the optimal OBJ value is equal to 0.203. As depicted in Fig. 1a, the *Log W* values predicted by NF-GMDH-GSA are limited to the lines corresponding to ±30% (i.e., predicted = 0.7 × measured, and predicted = 1.3 × measured). It is worth noting that more than 97.6% of all experimental results used in model development are limited to the lines corresponding to ±20%, indicating reasonable accuracy of the GMDH-based model in estimation of the strain energy required for initiation of liquefaction. Table 3 presents R^2, MAE, and RMSE values of the proposed strain energy model for the training, testing, and all datasets.

Moreover, for further investigation into the model's accuracy in predicting *Log W*, the difference between the measured and predicted values (residuals) was calculated and presented in Fig. 1b. As shown in this figure, the relative error of predicted *Log W* results is less than 0.6 J/m^3 and approximately 97% of the results had a relative error less than 0.4 J/m^3. Figure 1c also shows the plot of the normalized *Log W* (i.e., the ratio of the measured to the predicted *Log W* values) versus the predicted *Log W* values. The figure demonstrates that the average value of the normalized *Log W* is 0.995, which confirms that the predictions were unbiased. In addition, the minimum and the maximum values of normalized *Log W* were 0.80 and 1.19, respectively.

In order to confirm generality of the developed model, centrifuge test results from Dief (2000) were used as

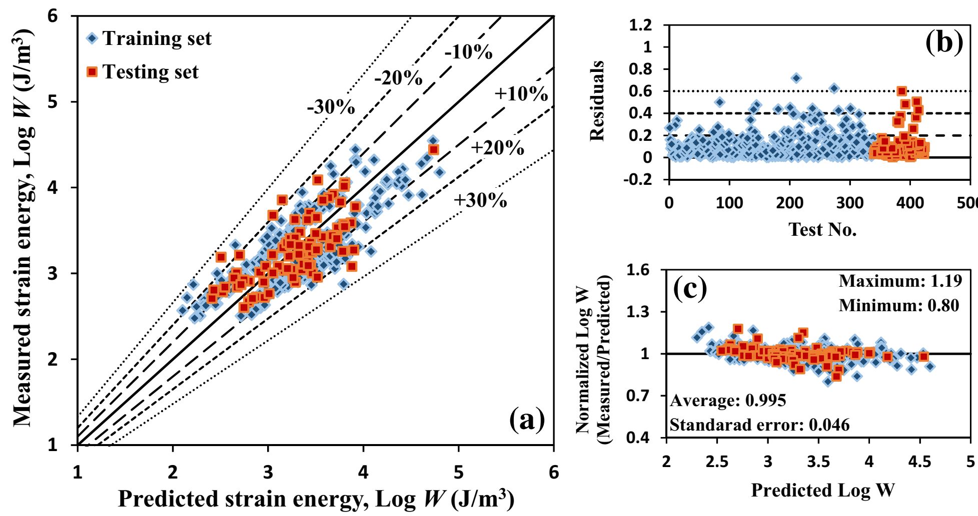

Fig. 1 **a** Measured values of strain energy versus group method of data handling–gravitational search algorithm (GMDH-GSA)-based predicted values for training and testing datasets; **b** histogram of the residuals; and **c** normalized *Log W* versus predicted *Log W* values. *Log W* strain energy values

validation testing set. Dief (2000) carried out these tests (Table 1) on Nevada, Reid Bedford, and LSFD sands. Figure 2 depicts predicted versus measured strain energy values for the centrifuge validation dataset. The R^2, MAE, and RMSE values of the developed model for this dataset were calculated as being equal to 0.733, 0.081, and 0.098, respectively (Table 3). In reality, the developed NF-GMDH-GSA-based model has obtained sufficient precision for both testing and validation sets.

Sensitivity analysis

The sensitivity analysis was conducted to investigate (i) how each parameter affects the strain energy needed for soil liquefaction occurrence; and (ii) the compliance of NF-GMDH-GSA performance with the experimental results to ensure the physical behavior of the developed model. To this end, the effect of changes in each input parameter on the amount of strain energy was investigated, while other parameters were assumed constant at their mean values in the database (Table 2). The strain energy (W) changes with D_r, σ'_0, FC, D_{50}, and C_u are presented in Figs. 3a–e, respectively.

Table 3 Accuracy of the *Log W* model for the training, testing, all data, and validation sets

Dataset	Number of data	Performance		
		R^2	MAE	RMSE
Training	339	0.937	0.024	0.036
Testing	85	0.883	0.040	0.051
All element tests	424	0.924	0.027	0.039
Validation (centrifuge tests)	22	0.733	0.181	0.198

Log W strain energy values, *MAE* mean absolute error, R^2 coefficient of determination, *RMSE* root mean squared error

Figure 3a–e also present a diagram of the *Log W* value with respect to each effective parameter for all cyclic experimental results (Table 1) used in model development along with their best fitted curve.

According to Figs. 3a and b, strain energy (W) increases with increasing σ'_0 and D_r. This finding is consistent with experimental studies of Lee and Seed (1967) and Figueroa et al. (1994). An increase in FC first increased and then decreased W (Fig. 3c). Although some researchers (e.g., Chien et al. 2002) have reported a decrease in liquefaction resistance as FC increases, Carraro et al. (2003), Polito and Martin (2001), and Hazirbaba and Rathje (2009) have reported an initial increase and subsequently a decrease in liquefaction resistance with increasing FC. W decreased by increasing C_u (Fig. 3d). In addition, W increased by increasing D_{50} (Fig. 3e). Liang (1995) showed that coarse-grained soils need a greater amount of strain energy than fine-grained soils for initiation of liquefaction. In general, comparison of changes in W when subjected to the most important parameters affecting the strain energy required for incidence of liquefaction with experimental studies (Figs. 3a–e) indicated the accuracy of the proposed GMDH-based model.

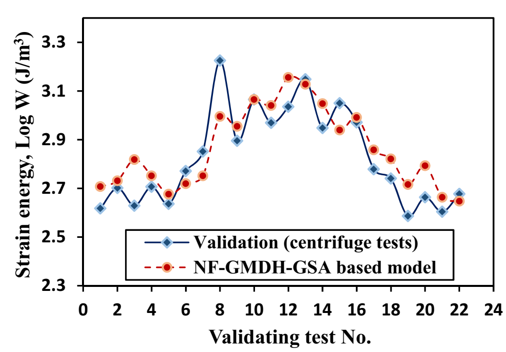

Fig. 2 Predicted strain energy versus measured values for the centrifuge validation dataset. *Log W* strain energy values, *NF-GMDH-GSA* neuro-fuzzy group method of data handling–gravitational search algorithm

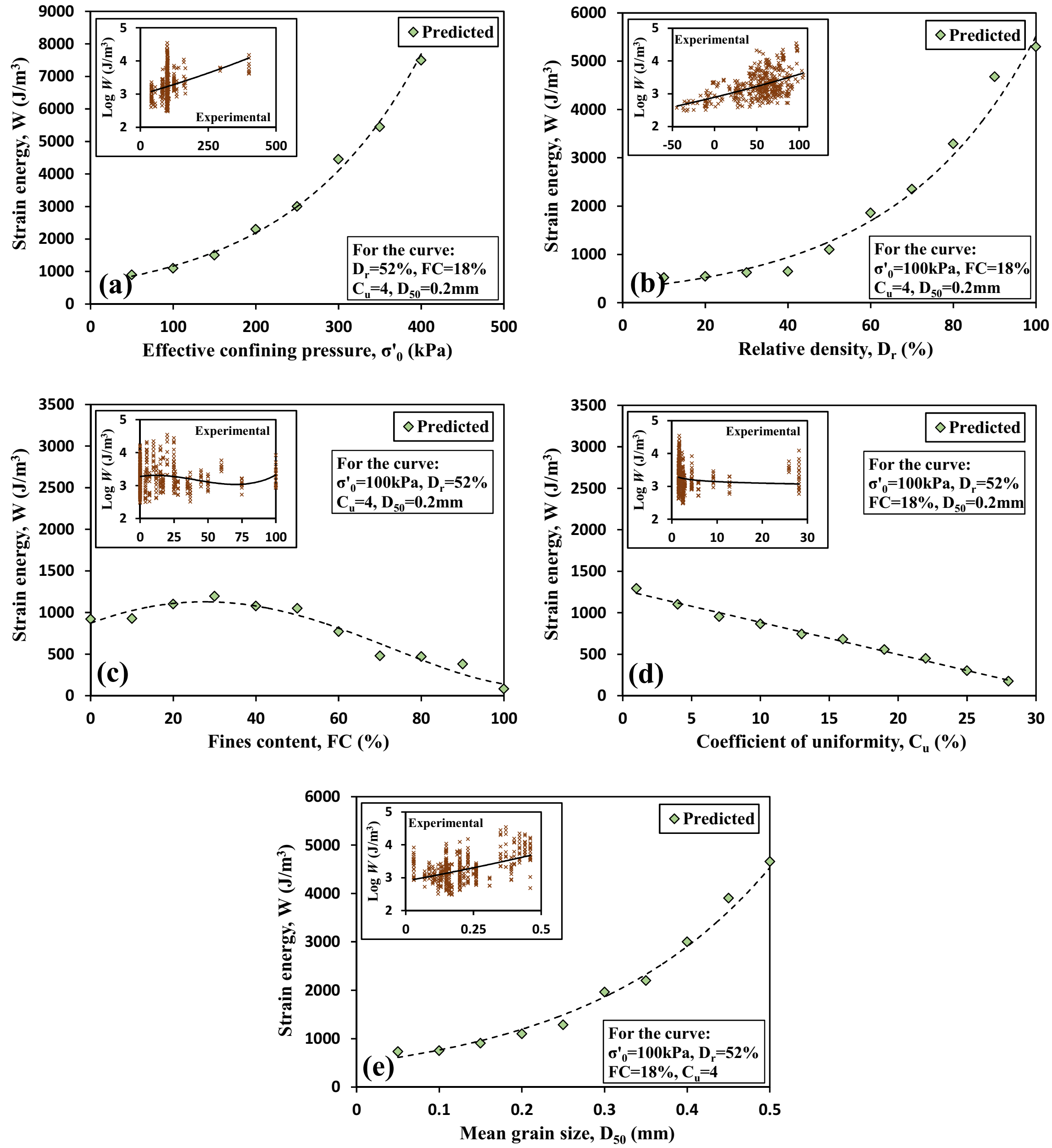

Fig. 3 Variation of the strain energy required for liquefaction onset predicted by a neuro-fuzzy group method of data handling–gravitational search algorithm (NF-GMDH-GSA)-based model against (**a**) σ'_0, (**b**) D_r, (**c**) FC, (**d**) C_u, and (**e**) D_{50}; gathered experimental data are also superimposed in the figures.
C_u coefficient of uniformity, D_{50} mean particle size, D_r relative density after consolidation, FC fines content, W strain energy, σ'_0 confining pressure

Experimental verification

Within the scope of this study, in order to verify NF-GMDH-GSA, a series of isotropically consolidated undrained (CU) cyclic triaxial laboratory tests were carried out on reconstituted samples of the sandy and silty sandy soils attained from the Khuzestan province in Iran. The particle size distribution curves of the tested soil specimens are depicted in Fig. 4. The soils are classified as poorly graded sand (Marandi and Javdanian 2012) according to the ASTM D2487. The maximum void ratio (e_{max}), minimum void ratio (e_{min}), and specific gravity (G_s) of the tested sands were measured in accordance with ASTM D4253, ASTM D4254, and ASTM D854, respectively. Figure 4 also presents some physical properties of the soils used in the present research.

The under-compaction procedure was used to prepare the soil specimens (Ladd 1978). All soil specimens were saturated with running water through the specimen. The controlling measure for full saturation was Skempton's saturation parameter $B = 0.95 - 1$. The height and the diameter of the specimens were 100 and 50 mm, respectively. Strain-controlled cyclic tests with the single strain amplitude of 0.5% were

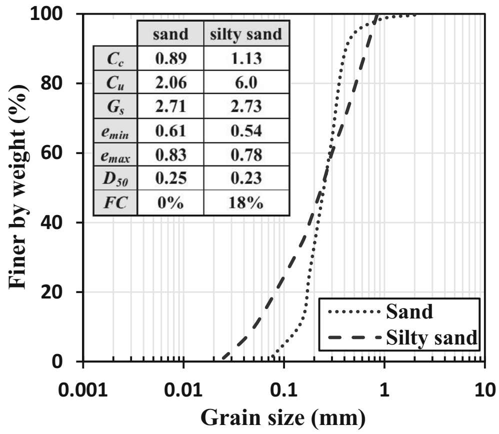

	sand	silty sand
C_c	0.89	1.13
C_u	2.06	6.0
G_s	2.71	2.73
e_{min}	0.61	0.54
e_{max}	0.83	0.78
D_{50}	0.25	0.23
FC	0%	18%

Fig. 4 Grain size distribution and physical properties of the tested soils. C_c coefficient of curvature, C_u coefficient of uniformity, D_{50} mean particle size, e_{max} maximum void ratio, e_{min} minimum void ratio, FC fines content, G_s specific gravity

conducted on each soil specimen. Each cyclic test was continued until the initial liquefaction happened. It is noteworthy that the initial liquefaction was supposed to happen when the excess pore water pressure became identical to the initial confining pressure ($r_u = 1$). The tests were conducted at confining pressures (σ'_0) of 50 and 100 kPa and relative densities after consolidation (D_r) of approximately 40% and 70%. The test series are summarized in Table 4, in which N_l is the number of cycles needed to liquefaction onset.

Axial loads, vertical displacements, and excess pore water pressures were measured during the cyclic tests. The measured axial strain amplitude (ε) was converted to shear strain amplitude (γ) using $\gamma = 1.5\varepsilon$, which assumes the Poisson's ratio (ν) of 0.5 for an undrained loading condition (Ishihara 1996; Jafarian et al. 2015; Jafarian et al. 2016a, 2016b; Jafarian and Javdanian 2017). Typical results of the experiment conducted on a silty sandy specimen at $\sigma'_0 = 50$ kPa and $D_r = 38.6\%$ are illustrated in Figs. 5a–e. These figures demonstrate the shear stress–strain curve (hysteresis loops) (Fig. 5a), history of excess pore water pressure (r_u) (Fig. 5b), history of cyclic shear strain (Fig. 5c), history of cyclic shear stress (Fig. 5d), and stress-path diagram (Fig. 5e).

The dissipated energy per volume (J/m^3) was determined by computing the inter area of the hysteresis loop (shear stress–shear strain curve) during a cycle of test. The dissipated strain energy until the soil liquefaction onset may be computed using Eq. 17:

$$\Delta w = \frac{1}{2}\sum_{i=1}^{n}\left(\tau_{d,i+1} + \tau_{d,i}\right)\left(\gamma_{a,i+1} - \gamma_{a,i}\right) \tag{17}$$

where Δw is the accumulative dissipated strain energy per soil volume up to liquefaction triggering, $\tau_{d,i}$ is the shear stress difference in the ith recorded point, n is the recorded points up to liquefaction occurrence, and $\gamma_{a,i}$ is the shear strain difference in the ith recorded point (Green 2001; Baziar and Sharafi 2011).

Table 4 Summary of the cyclic triaxial tests conducted on sands in this research

Soil	D_r (%)	σ'_0 (kPa)	N_l	W (J/m^3)
Sand	40.3	50	25.6	516
	40.1	100	40.7	1351
	68.7	50	33.2	885
	70.4	100	57.6	2671
Silty sand	38.6	50	26.8	497
	41.5	100	46.1	1437
	69.2	50	36.3	902
	73.1	100	64.9	2804

D_r relative densities after consolidation, N_l number of cycles needed to liquefaction onset, W strain energy, σ'_0 confining pressure

Calculated strain energy (W) up to liquefaction triggering in the cyclic triaxial tests on sandy and silty dandy soils are presented in Table 4. Comparison of cyclic triaxial tests results with values predicted by NF-GMDH-GSA is demonstrated in Fig. 6. As seen in this figure, the proposed model has good accuracy in prediction of the strain energy required for soil liquefaction onset ($R^2 = 0.701$, MAE = 0.126, RMSE = 0.147). It is worth noting that the model is more accurate in estimation of the energy required for liquefaction onset in sandy soil ($R^2 = 0.734$, MAE = 0.112, RMSE = 0.135) than in silty sand ($R^2 = 0.671$, MAE = 0.141, RMSE = 0.158) specimens.

Field verification

The data recorded during real earthquakes has been used to check the accuracy of the developed model under field conditions. On the basis of data from different earthquakes and using methodology followed by Davis and Berrill (1998), Butterfield (2004) calculated the stress and strain time histories and subsequently the history of dissipated strain energy in soil deposits. This amount of strain energy is known as released strain energy by earthquake source to a special site. The value of energy allotted to the soil deposit in a liquefiable site (which is imparted by an earthquake) should be greater than the predicted strain energy needed for liquefaction onset (which is assessed using the developed NF-GMDH-GSA-based model), and vice versa.

The amounts of released strain energy from an earthquake in several sites (Butterfield 2004) are used for field verification in our research. These sites at which the average stress and strain were assessed included the Sunamachi site (situated on a reclaimed peninsula immediately beside the estuary of the Ara River in Tokyo Bay, Japan) during the 1987 Chiba-Toho-Oki earthquake, Lotung Large Scale Seismic Test (LSST) (situated on the Lanyang plain, near the city of Lotung in northeast Taiwan) during the 1986 Event 16

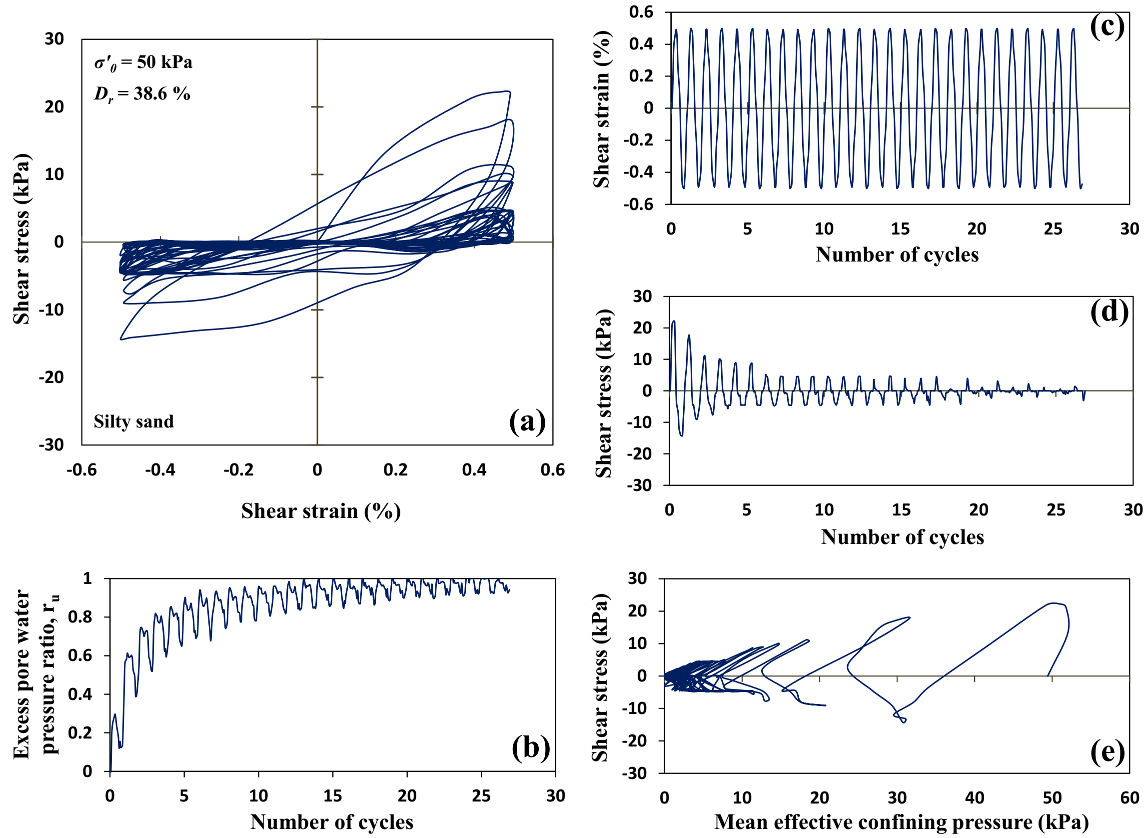

Fig. 5 Results of test on a silty sand specimen with $\sigma'_0 = 50$ kPa and $D_r = 38.6\%$. **a** Hysteretic shear stress–strain curve; **b** excess pore water pressure; **c** cyclic shear strain; **d** cyclic shear stress; and *e* stress-path diagram. D_r relative densities after consolidation, σ'_0 confining pressure

earthquake, and Wildlife Refuge Array of Imperial Valley (situated on the flood plain of the Alamo River in Imperial County, Southern California, USA) during the 1987 Superstition Hills earthquake. Available research indicates that liquefaction occurred during the Superstition Hills earthquake in the Wildlife Refuge Array of Imperial Valley

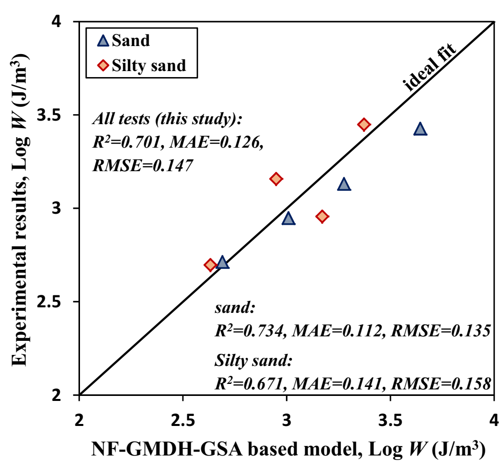

Fig. 6 Measured values of strain energy using cyclic triaxial tests in this study versus neuro-fuzzy group method of data handling–gravitational search algorithm (NF-GMDH-GSA)-based predicted values. *Log W* strain energy values, *MAE* mean absolute error, R^2 coefficient of determination, *RMSE* root mean squared error

(Butterfield 2004). Also, the pore pressure generated during the Chiba-Toho-Oki earthquake in Sunamachi and the Event 16 earthquake in Lotung LSST shows that a liquefaction phenomenon was not accrued in these sites (Ishihara et al. 1989; Zeghal et al. 1995).

A comparison of the amount of strain energy released by earthquakes with the strain energy required for liquefaction (predicted by the developed NF-GMDH-GSA-based model) is presented in Fig. 7. Points above the bisector indicate that the amount of energy released by earthquakes exceeds the energy required for liquefaction and, therefore, these points represent liquefaction cases. On the other hand, points below the bisector indicate that the amount of energy released by an earthquake is less than the energy required for liquefaction and, therefore, these points represent non-liquefaction cases. As seen in Fig. 7, the developed strain energy model accurately forejudges between liquefied and non-liquefied conditions for all real cases.

Comparison with some available relationships

The proposed NF-GMDH-GSA-based strain energy model has been compared with some available relationships

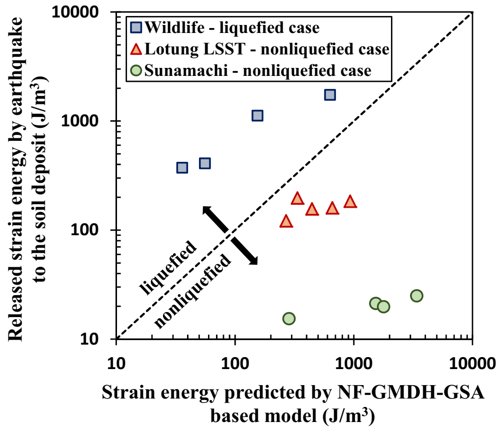

Fig. 7 Comparison of released strain energy by earthquake between the soil deposits and strain energy predicted by the neuro-fuzzy group method of data handling–gravitational search algorithm (NF-GMDH-GSA)-based model for various real sites. *LSST* Large Scale Seismic Test

(Figueroa et al. 1994; Liang 1995; Dief and Figueroa 2001; Baziar and Jafarian 2007; Alavi and Gandomi 2012) for evaluation of the strain energy required for liquefaction occurrence. Based on the results of the cyclic tests, Figueroa et al. (1994), Liang (1995), and Dief and Figueroa (2001) recommended various strain energy relationships using multiple linear regression (MLR). Baziar and Jafarian (2007) developed a MLR-based equation for estimation of *W* on the basis of a database of cyclic tests results. Alavi and Gandomi (2012) recommended a relationship for assessment of strain energy needed for liquefaction onset using linear genetic programming. The values of R^2, MAE, and RMSE for the developed NF-GMDH-GSA-based model and the aforementioned relationships for estimation of the strain energy required for liquefaction onset are presented in Table 5. The results presented in Table 5 confirm higher accuracy of the proposed NF-GMDH-GSA model than of the available recommendations.

Table 5 Comparison of the proposed model with previous studies

Model	Performance		
	R^2	MAE	RMSE
This study (all data)	0.924	0.027	0.039
Alavi and Gandomi (2012)	0.722	4.516	0.198
Baziar and Jafarian (2007)	0.592	4.237	0.312
Dief and Figueroa (2001)	0.348	4.347	0.462
Liang (1995)	0.329	6.358	0.475
Figueroa et al. (1994)	0.311	7.323	0.412

MAE mean absolute error, R^2 coefficient of determination, *RMSE* root mean squared error

Summary and conclusions

A wide-ranging database of cyclic experiments on sandy soils and silty sands was gathered in this study. Most important parameters affecting strain energy (*W*) required for liquefaction occurrence were determined through literature review and by studying soil behavior in different conditions. A model was developed using NF-GMDH and GSA to estimate *W*. Assessing the accuracy of developed model indicates high accuracy of the NF-GMDH-GSA-based model in estimation of the strain energy ($R^2 = 0.924$, MAE = 0.027, RMSE = 0.039). Comparison of strain energy results from centrifuge tests with predicted values confirmed reasonable accuracy of the developed model. The sensitivity analysis was performed to investigate the effect of each parameter on the amount of *W* and to ensure the behavior of the developed model. The *W* increased by increasing σ'_0, D_r, and D_{50}. In addition, *W* decreased by increasing C_u. An increase in *FC* first increased and then decreased *W*. Generally, the changes in *W* when subjected to the most important parameters affecting *W* were consistent with experimental tests results.

An experimental program was scheduled to assess the accuracy of developed NF-GMDH-GSA model in laboratory conditions. For this purpose, cyclic triaxial tests were carried out on two types of soil, namely sandy soil and silty soil. The cyclic tests were conducted under various effective confining pressures and relative densities. The amount of strain energy dissipated until liquefaction onset ($r_u = 1$) was calculated using the hysteresis loops. Comparison of strain energy results from experiments and predicted values indicated its acceptable accuracy. The amounts of energy released by real earthquakes in different areas were used for field verification of the proposed model. The ability of the NF-GMDH-GSA model to distinguish liquefied areas from non-liquefied ones reflects its reasonable accuracy in field conditions. Comparison with available relationships confirms satisfactory performance of the proposed model. Certainly, further experiments under different conditions being conducted could improve the performance of strain energy-based models for estimation of soil liquefaction potential. However, this will require further research on the liquefaction phenomenon.

Acknowledgements This work has been financially supported by the research deputy of Shahrekord University (grant number 95GRN1M39422). This support is gratefully acknowledged. Special thanks are also extended to engineers from the Dez Shaloudeh Azma Co., Iran, for providing laboratory facilities.

References

Alavi AH, Gandomi AH (2012) Energy-based numerical models for assessment of soil liquefaction. Geosci Front 3(4):541–555

Arulmoli K, Muraleetharan KK, Hosain MM, Fruth LS (1992) VELACS laboratory testing program. Soil Data Report, The Earth Technology Corporation, Irvine, Calif. Report to the National Science Foundation, Washington, DC

Baziar MH, Dobry R (1995) Residual strength and large-deformation potential of loose silty sands. J Geotech Eng ASCE 121(12):896–906

Baziar MH, Jafarian Y (2007) Assessment of liquefaction triggering using strain energy concept and ANN model: capacity energy. Soil Dyn Earthq Eng 27(12):1056–1072

Baziar MH, Sharafi H (2011) Assessment of silty sand liquefaction potential using hollow torsional tests—an energy approach. Soil Dyn Earthq Eng 31(7):857–865

Baziar MH, Jafarian Y, Shahnazari H, Movahed V, Tutunchian MA (2011) Prediction of strain energy-based liquefaction resistance of sand–silt mixtures: an evolutionary approach. Comput Geosci 37(11):1883–1893

Butterfield KJ (2004) Seismic liquefaction trigger mechanisms. PhD Dissertation, Department of Civil Engineering, University of Canterbury

Caglar N, Arman H (2007) The applicability of neural networks in the determination of soil profiles. Bull Eng Geol Environ 66(3):295–301

Carraro JAH, Bandini P, Salgado R (2003) Liquefaction resistance of clean and nonplastic silty sands based on cone penetration resistance. J Geotech Geoenviron Eng ASCE 129(11):965–976

Chien LK, Oh YN, Chang CH (2002) Effects of fines content on liquefaction strength and dynamic settlement of reclaimed soil. Can Geotech J 39:254–265

Davis RO, Berrill JB (1998) Rational approximation of shear stress and strain based on downhole acceleration measurements. Int J Numer Anal Meth Geomech 22:603–619

Dief HM (2000) Evaluating the liquefaction potential of soils by the energy method in the centrifuge. PhD Dissertation, Department of Civil Engineering, Case Western Reserve University, Cleveland

Dief HM, Figueroa JL (2001) Liquefaction assessment by the energy method through centrifuge modeling. In: Zeng XW (ed) Proceedings of the NSF international workshop on earthquake simulation in geotechnical engineering. CWRU, Cleveland

Dobry R, Ladd RS, Yokel FY, Chung RM, Powell D (1982) Prediction of pore water pressure build-up and liquefaction of sands during earthquakes by the cyclic strain method. National Bureau of Standards, US Department of Commerce, US Governmental Printing Office, Building Science Series, Washington, DC

Figueroa JL, Saada AS, Liang L, Dahisaria NM (1994) Evaluation of soil liquefaction by energy principles. J Geotech Eng ASCE 120(9): 1554–1569

Gandomi AH, Babanajad SK, Alavi AH, Farnam Y (2012) Novel approach to strength modeling of concrete under triaxial compression. J Mater Civ Eng 24(9):1132–1143

Goh AT, Zhang WG (2014) An improvement to MLR model for predicting liquefaction-induced lateral spread using multivariate adaptive regression splines. Eng Geol 170:1–10

Green RA (2001) Energy-based evaluation and remediation of liquefiable soils. PhD dissertation, Virginia Polytechnic Institute and State University, Blacksburg

Hazirbaba K, Rathje EM (2009) Pore pressure generation of silty sands due to induced cyclic shear strains. J Geotech Geoenviron Eng ASCE 135(12):1892–1905

Hwang HS (2006) Fuzzy GMDH-type neural network model and its application to forecasting of mobile communication. Comput Ind Eng 50(4):450–457

Ishihara K (1996) Soil behavior in earthquake geotechnics. Oxford Science Publications

Ishihara K, Muroi T, Towhata I (1989) In-situ pore water pressures and ground motions during the 1987 Chiba-Toho-Oki earthquake. Soils Found 29(4):75–90

Jafarian Y, Javdanian H (2017) Dynamic behavior of calcareous sands. Bull Earthq Sci Eng 4(1):27–36

Jafarian Y, Sadeghi Abdollahi A, Vakili R, Baziar MH (2010) Probabilistic correlation between laboratory and field liquefaction potentials using relative state parameter index. Soil Dyn Earthq Eng 30:1061–1072

Jafarian Y, Sadeghi Abdollahi A, Vakili R, Baziar MH, Noorzad A (2011) On the efficiency and predictability of strain energy for the evaluation of liquefaction potential: a numerical study. Comput Geotech 38(6):800–808

Jafarian Y, Towhata I, Baziar MH, Noorzad A, Bahmanpour A (2012) Strain energy based evaluation of liquefaction and residual pore water pressure in sands using cyclic torsional shear experiments. Soil Dyn Earthq Eng 35:13–28

Jafarian Y, Haddad A, Javdanian H (2014) Predictive model for normalized shear modulus of cohesive soils. Acta Geodyn Geomater 11(1): 89–100

Jafarian Y, Haddad A, Javdanian H (2015) Comparing the shear stiffness of calcareous and silicate sands under dynamic and cyclic straining. 7th Int Conf Seismol Earthq Eng (SEE7), 18 May, Tehran

Jafarian Y, Javdanian H, Haddad A (2016a) Comparing dynamic behavior of Hormuz calcareous and Babolsar siliceous sands under identical conditions. Bull Earthq Sci Eng 3(3):1–10

Jafarian Y, Haddad A, Javdanian H (2016b) Estimating the shearing modulus of Boushehr calcareous sand using resonant column and cyclic triaxial experiments. Modares Civil Eng J 15(4):9–19

Javdanian H (2017) Assessment of shear stiffness ratio of cohesionless soils using neural modeling. Model Earth Syst Environ 3(3):1045–1053

Javdanian H (2017) The effect of geopolymerization on the UCS of stabilized fine-grained soils. Int J Eng Trans B Appl 30(11):1508–1517

Javdanian H, Hoseini O (2016) Evaluating performance of the existing relationships and models to predict liquefaction-induced lateral spreading. 5th Int Conf Geotech Eng Soil Mech, 15 November, Tehran

Javdanian H, Seidali M (2016) Evaluating liquefaction induced lateral spreading. 5th Int Conf Geotech Eng Soil Mech, 15 November, Tehran

Javdanian H, Haddad A, Mehrzad B (2012) Experimental and numerical investigation of the bearing capacity of adjacent footings on reinforced soil. Electronic J Geotech Eng 17(R):2597–2617

Javdanian H, Haddad A, Jafarian A (2015a) Evaluation of dynamic behavior of fine-grained soils using group method of data handling. Transp Infrastruct Eng 1(3):77–92. http://jtie.journals.semnan.ac.ir/article_318_en.html

Javdanian H, Jafarian Y, Haddad A (2015b) Predicting damping ratio of fine-grained soils using soft computing methodology. Arab J Geosci 8(6):3959–3969

Javdanian H, Heidari A, Kamgar R (2017) Energy-based estimation of soil liquefaction potential using GMDH algorithm. Iran J Sci Technol Trans Civ Eng 41(3):283–295

Kalantary F, Ardalan H, Nariman-Zadeh N (2009) An investigation on the S_u-N_{SPT} correlation using GMDH type neural networks and genetic algorithms. Eng Geol 104:144–155

Kanagalingam T (2006) Liquefaction Resistance of Granular Mixes Based on Contact Density and Energy Considerations. PhD Dissertation, The State University of New York at Buffalo, Buffalo

Kaveh A, Hamze-Ziabari SM, Bakhshpoori T (2016) Patient rule-induction method for liquefaction potential assessment based on CPT data. Bull Eng Geol Environ. https://doi.org/10.1007/s10064-016-0990-3

Kokusho T, Mimori Y (2015) Liquefaction potential evaluations by energy-based method and stress-based method for various ground motions. Soil Dyn Earthq Eng 75:130–146

Ladd RS (1978) Preparing test specimens using undercompaction. Geotech Test J 1(1):16–23

Lee KL, Fitton JA (1968) Factors affecting the cyclic loading strength of soil. Vibration Effects of Earthquakes on Soils and Foundation, ASTM STP 450, American Society for Testing and Materials. 71–95

Lee KL, Seed HB (1967) Cyclic stress conditions causing liquefaction of sand. J Soil Mech Found Div ASCE 93(SM1):47–70

Li X, Zhong D, Ren B, Fan G, Cui B (2017) Prediction of curtain grouting efficiency based on ANFIS. Bull Eng Geol Environ. https://doi.org/10.1007/s10064-017-1039-y

Liang L (1995) Development of an energy method for evaluating the liquefaction potential of a soil deposit. PhD Dissertation, Department of Civil Engineering, Case Western Reserve University, Cleveland

Madala HR, Ivakhnenko AG (1994) Inductive learning algorithms for complex systems modeling. CRC Press, Boca Raton

Marandi SM, Javdanian H (2012) Laboratory studies on bearing capacity of strip interfering shallow foundations supported by geogrid-reinforced sand. Adv Mater Res 472:1856–1869

Mehrzad B, Haddad A, Jafarian Y (2016) Centrifuge and numerical models to investigate liquefaction-induced response of shallow foundations with different contact pressures. Int J Civ Eng 14(2): 117–131

Mohammadi SD, Naseri F, Alipoor S (2015) Development of artificial neural networks and multiple regression models for the NATM tunnelling-induced settlement in Niayesh subway tunnel, Tehran. Bull Eng Geol Environ 74(3):827–843

Naeini SA, Baziar MH (2004) Effect of fines content on steady-state strength of mixed and layered samples of a sand. Soil Dyn Earthq Eng 24:181–187

Najafzadeh M, Azamathulla HM (2013) Neuro-fuzzy GMDH systems to predict the scour pile groups due to waves. J Comput Civ Eng. https://doi.org/10.1061/(ASCE)CP.1943-5487.0000376

Najafzadeh M, Lim SY (2014) Application of improved neuro-fuzzy GMDH to predict scour downstream of sluice gates. Earth Sci Inform 8(1):187–196

Najafzadeh M, Tafarojnoruz A (2016) Evaluation of neuro-fuzzy GMDH-based particle swarm optimization to predict longitudinal dispersion coefficient in rivers. Environ Earth Sci 75(2):157

Najafzadeh M, Barani GA, Hessami Kermani MR (2013) GMDH network based back propagation algorithm to predict abutment scour in cohesive soils. Ocean Eng 59:100–106

Papathanassiou G, Seggis K, Pavlides S (2011) Evaluating earthquake-induced liquefaction in the urban area of Larissa, Greece. Bull Eng Geol Environ 70(1):79–88

Polito CP, Martin JR (2001) Effects of nonplastic fines on the liquefaction resistance of sands. J Geotech Geoenviron Eng ASCE 127(5):408–415

Rahman MZ, Siddiqua S (2017) Evaluation of liquefaction-resistance of soils using standard penetration test, cone penetration test, and shear-wave velocity data for Dhaka, Chittagong, and Sylhet cities in Bangladesh. Environ Earth Sci 76(5):207

Rashedi E, Nezamabadipour H, Saryazdi S (2009) GSA: a gravitational search algorithm. Inf Sci 179:2232–2248

Rokoff MD (1999) The influence of grain-size characteristics in determining the liquefaction potential of a soil deposit by the energy method. MSc Dissertation, Department of Civil Engineering, Case Western Reserve University, Cleveland

Seed HB, Idriss IM (1971) Simplified procedure for evaluating soil liquefaction potential. J Soil Mech Found Div 97:1249–1273

Seed HB, Lee KL (1966) Liquefaction of saturated sands during cyclic loading. J soil Mech found div ASCE 92(SM2);105–134

Shahin MA, Maier HB, Jaksa MB (2004) Data division for developing neural networks applied to geotechnical engineering. J Comput Civ Eng ASCE 18(2):105–114

Sonmez B, Ulusay R (2008) Liquefaction potential at Izmit Bay: comparison of predicted and observed soil liquefaction during the Kocaeli earthquake. Bull Eng Geol Environ 67(1):1–9

Takashi O, Hidetomo I, Tetsuya M, Kazunori N (1998) Orthogonal and successive projection methods for the learning of neurofuzzy GMDH. Inf Sci 110:5–24

Tao M (2003). Case history verification of the energy method to determine the liquefaction potential of soil deposits. PhD Dissertation, Department of Civil Engineering, Case Western Reserve University, Cleveland

Thevanayagam S (1998) Effect of fines and confining stress on undrained shear strength of silty sands. J Geotech Geoenviron Eng ASCE 124(6):479–491

Towhata I (1986) Discussion to “energy dissipation and seismic liquefaction of sands: revised model” by Berrill JB, Davis RO. Soils Found 26(1):134–135

Towhata I, Ishihara K (1985) Shear work and pore water pressure in undrained shear. Soils Found 25(3):73–84

Whitman RV (1971) Resistance of soil to liquefaction and settlement. Soils Found 11(4):59–68

Xue X, Yang X (2016) Seismic liquefaction potential assessed by support vector machines approaches. Bull Eng Geol Environ 75(1):153–162

Youd T, Idriss I, Andrus R, Arango I, Castro G, Christian J, Dobry R, Finn W, Harder LJ, Hynes M, Ishihara K, Koester J, Liao S, Marcuson W, Martin G, Mitchell J, Moriwaki Y, Power M, Robertson P, Seed R, Stokoe K II (2001) Liquefaction resistance of soils: summary report from the 1996 NCEER and 1998 NCEER/NSF workshops on evaluation of liquefaction resistance of soils. J Geotech Geoenviron Eng 127(10):817–833

Zeghal M, Elgamal AW, Tang HT, Stepp JC (1995) Lotung downhole array. II: evaluation of soil nonlinear properties. J Geotech Eng ASCE 121(4):363–378

Zhang WG, Goh ATC (2013) Multivariate adaptive regression splines for analysis of geotechnical engineering systems. Comput Geotech 48: 82–95

Zhang W, Goh AT (2016) Multivariate adaptive regression splines and neural network models for prediction of pile drivability. Geosci Front 7(1):45–52

Zhuang H, Chen G, Hu Z, Qi C (2016) Influence of soil liquefaction on the seismic response of a subway station in model tests. Bull Eng Geol Environ 75(3):1169–1182